INSTITUTE OF PHYSICS PUBLISHING JOURNAL OF PHYSICS A: MATHEMATICAL AND GENERAL

J. Phys. A: Math. Gen. **36** (2003) 5877–5885 PII: S0305-4470(03)55093-4

Simulations of strongly coupled charged particle systems: static and dynamical properties of classical bilayers

Zoltán Donkó[1], **Péter Hartmann**[1], **Gabor J Kalman**[2] **and Kenneth I Golden**[3]

[1] Research Institute for Solid State Physics and Optics, Hungarian Academy of Sciences, POB 49, H-1525 Budapest, Hungary
[2] Department of Physics, Boston College, Chestnut Hill, MA 02467, USA
[3] Department of Mathematics and Statistics, University of Vermont, Burlington, VT 05401, USA

Received 21 October 2002, in final form 29 January 2003
Published 22 May 2003
Online at stacks.iop.org/JPhysA/36/5877

Abstract

This paper reviews our recent molecular dynamics simulation studies of the static and dynamical behaviour of classical bilayers in their liquid phase. The pair correlation functions obtained in the static calculations make it possible to trace the structural changes of the system as well as to calculate the energy and static structure functions of the bilayer. The dynamical calculations show the existence of two (in-phase and out-of-phase) longitudinal and two (in-phase and out-of-phase) transverse collective modes. We present the full dispersion relations for these modes at different layer separations. At low layer separations the out-of-phase modes are found to possess a finite frequency at wave numbers $k \to 0$, confirming the existence of the long-wavelength energy gap in the bilayer system predicted by the quasi-localized charge approximation. It is only at higher layer separations that the dominant portion of the longitudinal out-of-phase mode is well approximated by the acoustic behaviour, resulting from the random phase approximation theory.

PACS numbers: 52.27.Gr, 52.65.−y, 05.20.−y, 73.21.−b

1. Introduction

Layered structures of charged particles can be realized in various physical systems, e.g., ion traps [1, 2], semiconductor devices [3–5] and complex (dusty) plasmas with mesoscopic charged grains [6–9]. Bilayers—consisting of two quasi two-dimensional layers of charged particles—represent the simplest form of multilayered systems. It has been shown both experimentally [1] and theoretically [10–14] that bilayers exhibit a rich variety of structural phases depending on the system parameters. Bilayers described through a model of classical

point charges interacting through the three-dimensional Coulomb potential can be fully characterized by two variables: (i) the coupling parameter $\Gamma = e^2/(akT)$, defined in the same manner as in the case of a single layer [15, 16], where $a = (n\pi)^{-1/2}$ is the Wigner–Seitz (WS) radius, n is the surface density of particles, and (ii) the separation of the two layers d/a.

The zero-temperature classical calculations of Goldoni and Peeters [17] have identified a sequence of structural changes (hexagonal $\rightarrow$ staggered rectangular $\rightarrow$ staggered square $\rightarrow$ staggered rhombic $\rightarrow$ staggered hexagonal) with increasing layer separation. The series of structural changes has also been observed by Weis *et al* through Monte Carlo (MC) simulations at nonzero temperature but still in the solid phase [18]. Theoretical calculations in the liquid phase have been carried out by Valtchinov *et al* [10, 11] and Kalman *et al* [12–14], using the hypernetted chain (HNC) technique [19]. These studies have shown that the series of structural changes also exists in the strongly coupled liquid phase. The solid–liquid phase diagram of the bilayer system has been determined by MC simulations by Schweigert *et al* [20, 21]. Their results indicate a substantial change of melting temperature with layer separation. The highest melting temperature was found for layer separations, where the system is in the staggered square phase. The appearance of the pronounced long-range order in this domain of d/a (as seen from the behaviour of the intralayer and interlayer pair correlation functions) [22] as well as the largely reduced self-diffusion coefficient [23] can also be attributed to the solidification of the system.

The dynamical properties of bilayers for the weakly coupled electron gas and for the strongly coupled solid and liquid phases have been studied theoretically. The random phase approximation (RPA) [24] has predicted an acoustic behaviour for the longitudinal out-of-phase mode. The description of the phonon spectrum of the bilayer crystal by Goldoni and Peeters [17] was followed by the analysis of the strongly coupled liquid phase with the aid of the quasi-localized charge approximation (QLCA) [25]. The QLCA analysis has revealed the existence of four distinct collective excitations [26]: the longitudinal in-phase and out-of-phase modes (particles in the two layers oscillating in phase and 180° out of phase, respectively), and the transverse in-phase and out-of-phase modes. The in-phase modes emulate a 2D behaviour while the out-of-phase modes exhibit qualitatively new features. The analysis shows that in sharp contrast to the results of the RPA theory, at low layer separation ($d < a$) this mode exhibits a nonzero frequency at wave numbers $k \rightarrow 0$ [26]. The matter of this energy gap has, however, become the subject of some controversy. The issues brought forward have been the possible effect of damping [27, 28] and the compatibility of the RPA and QLCA predictions [29, 30].

The simulations described in this paper have been carried out in order to provide a definitive answer to the questions relating to the phases and to the mode structure of the strongly coupled bilayer liquid. In the present work, we briefly review the details of the static simulations [22] and present for the first time molecular dynamics (MD) data for the intralayer and interlayer correlation energies. The dynamical simulations reported here represent a preliminary account of a more comprehensive work [31] to be published later. The simulation technique is described in section 2; the results of the static and dynamical simulations are presented in sections 3 and 4, respectively. A summary of the work is given in section 5.

2. Simulation technique

Our molecular dynamics simulations are based on the particle–particle particle-mesh (PPPM) method [32]. This method makes it possible to simulate large ensembles of particles interacting through long-range forces, and uses periodic boundary conditions. We apply

a two-dimensional variant of the algorithm and map the two layers into a single layer with interaction potentials:

$$\begin{bmatrix} \phi_{11} & \phi_{12} \\ \phi_{21} & \phi_{22} \end{bmatrix} = e^2 \begin{bmatrix} 1/r & 1/\sqrt{(r^2+d^2)} \\ 1/\sqrt{(r^2+d^2)} & 1/r \end{bmatrix}. \tag{1}$$

In the simulations presented here the number of particles is set to $N = 1600$ in both layers, and we investigate the domain $10 \leqslant \Gamma \leqslant 80$ and $0 \leqslant d/a \leqslant 3$. The principal results of the static simulations are the intralayer $g_{11}(r/a)$ and interlayer $g_{12}(r/a)$ pair correlation functions (PCF). The potential energy of the system and the static structure functions are derived from g_{11} and g_{12}. The intralayer (E_{11} and E_{22} for layers 1 and 2, respectively) as well as interlayer (E_{12}) contributions to the potential energy of the whole system are given by

$$E_{11} = E_{22} = N\frac{e^2}{a^2}\int_0^\infty [g_{11}(r) - 1]\,\mathrm{d}r \tag{2}$$

and

$$E_{12} = 2N\frac{e^2}{a^2}\int_0^\infty \frac{r}{\sqrt{r^2+d^2}}[g_{12}(r) - 1]\,\mathrm{d}r. \tag{3}$$

The total potential energy per particle is $E/(2N) = (E_{11} + E_{12} + E_{22})/(2N) = (2E_{11} + E_{12})/(2N)$, as $E_{11} = E_{22}$.

The intralayer and interlayer structure functions are calculated through the Hankel transform of the pair correlation functions

$$S_{11}(k) = 1 + 2\pi n\int_0^\infty [g_{11}(r) - 1]r\,J_0(kr)\,\mathrm{d}r \tag{4}$$

$$S_{12}(k) = 2\pi n\int_0^\infty [g_{12}(r) - 1]r\,J_0(kr)\,\mathrm{d}r \tag{5}$$

where J_0 is the zeroth-order Bessel function.

The dynamical properties are investigated through the spectra of the correlations in the longitudinal and transverse current fluctuations, $L(k,\omega)$ and $T(k,\omega)$, respectively, and in the density fluctuations $S(k,\omega)$ (e.g., [33]). For the bilayer system we calculate $L_\pm(k,\omega)$, $T_\pm(k,\omega)$ and $S_\pm(k,\omega)$, where the + and − signs refer to the in-phase and out-of-phase modes, respectively [31].

3. Static properties

The dependence of the intralayer and interlayer pair correlation functions on the layer separation (d/a) is illustrated in figure 1 for $\Gamma = 50$. At $d/a = 0$—as the two layers merge into a single layer—g_{11} and g_{12} are identical. Here the system is in a hexagonal phase, however, a substitutional disorder occurs: some of the lattice sites corresponding to one of the layers are occupied by particles belonging to the other layer. This substitutional disorder gradually disappears with increasing d/a [22].

As the layer separation is increased both g_{11} and g_{12} exhibit significant changes. Examining the snapshots of particle positions and intralayer and interlayer coordination numbers [22], the sequence of structural changes (similar to the zero-temperature case) can be traced. The two layers become uncorrelated at separations exceeding $\sim 2a$, g_{11} in this domain corresponds to a single separated layer of charges. The correlation between the two layers is the strongest at layer separations $0.5 \leqslant d/a \leqslant 0.8$ as indicated by the amplitude

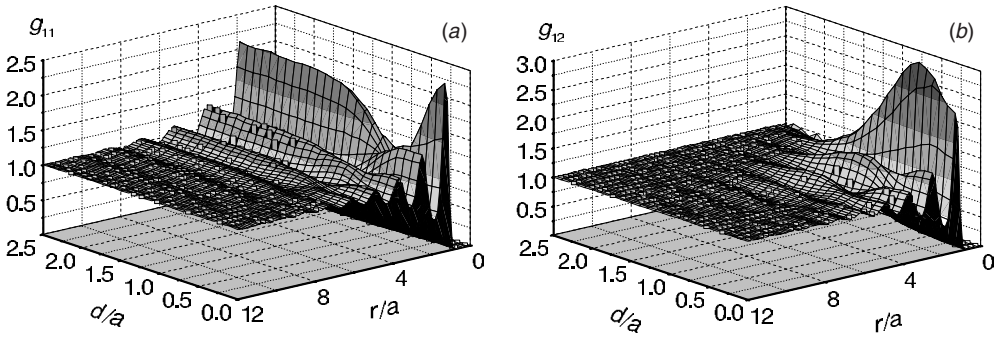

Figure 1. Intralayer (*a*) and interlayer (*b*) pair correlation functions for $\Gamma = 50$. Note the strong interlayer correlation in the domain $0.5 \leqslant d/a \leqslant 1$.

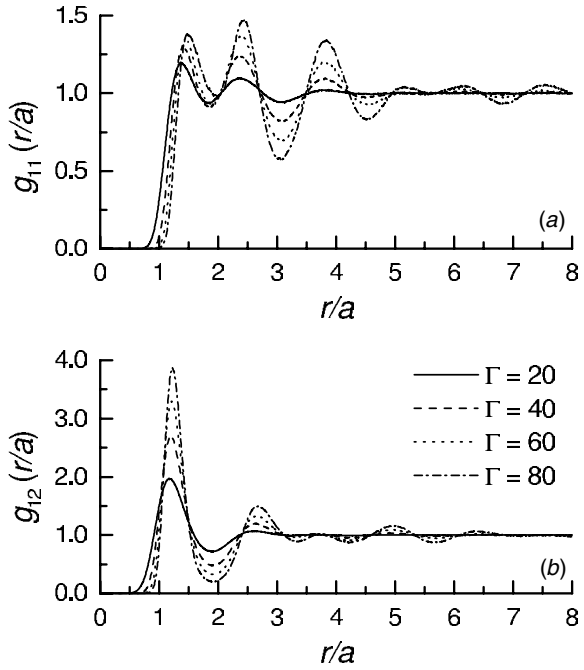

Figure 2. Intralayer (*a*) and interlayer (*b*) pair correlation functions for fixed layer separation $d/a = 0.5$ and different values of the coupling parameter. The positions of the minima and maxima change only slightly with decreasing Γ, demonstrating the stability of the structure.

of the first peak of g_{12}. The emergence of long-range order in this domain of d/a at higher values of coupling (e.g., $\Gamma = 80$) is a sign of the freezing of the bilayer into a crystal under these conditions. According to the studies by Scheweigert *et al* [20, 21], the freezing of the bilayer system occurs at the highest temperature in this domain of layer separations. (For the conditions of figure 1 the bilayer system is in a liquid state.)

At fixed layer separation the underlying structure in the liquid phase does not change with Γ. This is illustrated in figure 2, where g_{11} and g_{12} are plotted for a series of Γ values at a fixed layer separation ($d/a = 0.5$). It can clearly be seen that while the amplitudes of the peaks of

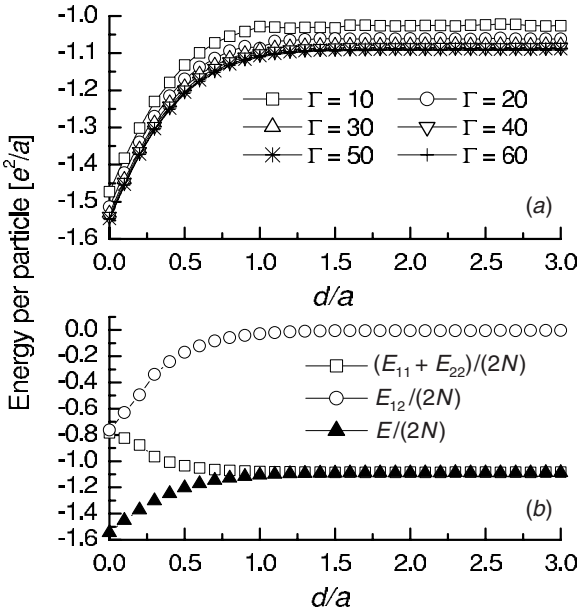

Figure 3. (*a*) The dependence of the total potential energy per particle $E/(2N)$ on d/a and Γ. (*b*) Intralayer $(E_{11} + E_{22})/(2N)$ and interlayer $E_{12}/(2N)$ contributions to the potential energy per particle and total potential energy per particle $E/(2N)$ as a function of layer separation (at $\Gamma = 50$). At high d/a the total energy approaches the Madelung energy for a hexagonal lattice. Appreciable interlayer energy is found at layer separations below $d/a \approx 1$.

the pair correlation functions get smaller as the coupling parameter decreases, the positions of the peaks remain nearly the same, thus proving the stability of the structure.

The potential energy per particle $E/(2N)$ is shown in figure 3(*a*) as a function of layer separation, for several values of Γ. In the high coupling limit at high layer separations the energy approaches the Madelung energy of a hexagonal lattice $E_M \cong -1.106e^2/a$ (e.g., [34]). At $d \to 0$, the energy approaches $E_M\sqrt{2}$, as the two layers transform into a single hexagonal lattice. For any fixed layer separation we find that the absolute value of the energy decreases towards lower values of Γ. The intralayer and interlayer contributions to the potential energy per particle, $(E_{11} + E_{22})/(2N)$ and $E_{12}/(2N)$, respectively, are plotted in figure 3(*b*). At $d = 0$, we find that $E_{11} + E_{22} = E_{12}$, as expected. At $d/a > 1$, the interlayer contribution becomes very small, and $(E_{11} + E_{22})/(2N)$ is approximately equal to the total energy.

The static structure functions $S_{11}(k)$ and $S_{12}(k)$ are plotted in figure 4, for $\Gamma = 20$ and a series of layer separations. The calculated structure functions satisfy the perfect screening sum rule $S_{11}(k = 0) = -S_{12}(k = 0) = S_0$. S_0 decreases rapidly with increasing layer separation.

4. Dynamical properties

Figure 5 shows the spectra of the longitudinal current fluctuations calculated at $\Gamma = 40$. The in-phase (L_+) and out-of-phase (L_-) spectra displayed in figures 5(*a*) and (*b*), respectively, have been obtained at $d/a = 0.3$, while figures 5(*c*) and (*d*) show L_+ and L_- spectra obtained at $d/a = 2.0$. All plots show spectra for eight values of the wave number, multiples of $(ka)_{\min} = 0.0886$. The results are displayed as a function of the ratio of oscillation frequency to the nominal 2D plasma frequency $\omega_0 = (2\pi ne^2/ma)^{1/2}$.

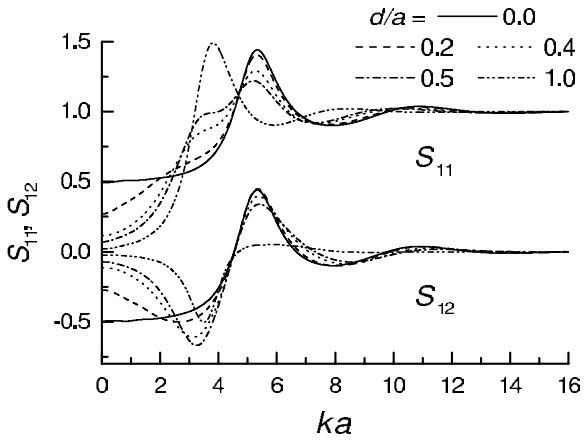

Figure 4. Static structure functions $S_{11}(k)$ and $S_{12}(k)$ for different values of layer separation, at $\Gamma = 20$. The $S_{11}(k)$ and $S_{12}(k)$ functions satisfy the perfect screening sum rule: $S_{11}(k = 0) = -S_{12}(k = 0)$.

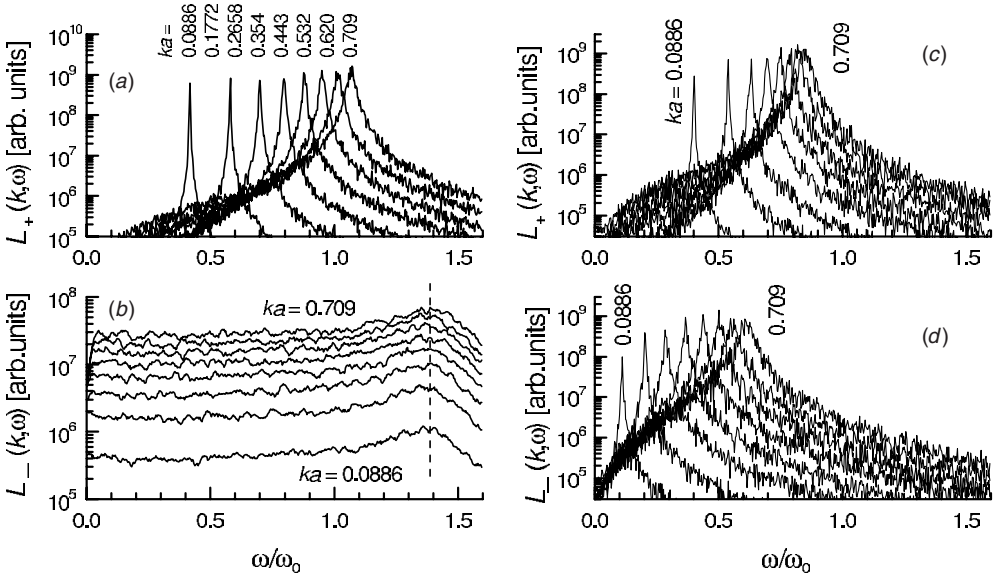

Figure 5. Spectra of the longitudinal current fluctuations at $\Gamma = 40$: (*a*) in-phase and (*b*) out-of-phase spectra at $d/a = 0.3$, (*c*) in-phase and (*d*) out-of-phase spectra at $d/a = 2.0$. The vertical dashed line in (*b*) marks the position of the gap.

For $d/a = 0.3$, the in-phase L_+ mode exhibits sharp peaks and a positive dispersion: the peaks are shifted towards higher ω with increasing k. The out-of-phase L_- mode, on the other hand, shows a very different behaviour: the peaks characterizing the collective excitation are quite broad, and remain at the same frequency at $k \to 0$. This behaviour provides direct evidence for the presence of an energy gap in the out-of-phase mode spectrum of a strongly coupled bilayer. The increased layer separation causes significant change only to the L_- mode spectra. At $d/a = 2$, we are no longer able to observe the energy gap; at this layer separation

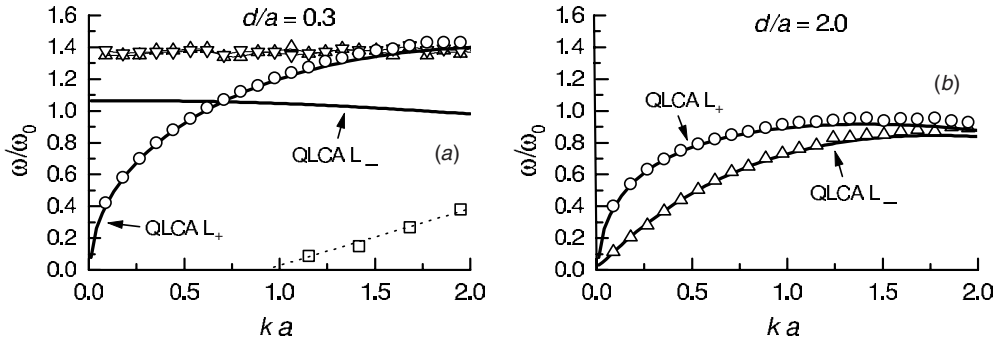

Figure 6. (*a*) Dispersion relations for the L_- ($\triangle$), T_- ($\triangledown$), L_+ ($\bigcirc$) and T_+ ($\square$) modes at $d/a = 0.3$. (*b*) Dispersion relations for the L_- ($\triangle$) and L_+ ($\bigcirc$) modes at $d/a = 2.0$. The heavy lines represent the QLCA results for the L_- and L_+ modes.

the collective excitations displayed in figure 5(*d*) are maintained by the mean field, rather than by the particle correlations.

The full dispersion relations $\omega(k)$ of the L modes obtained at $\Gamma = 40$ are plotted in figures 6(*a*) and (*b*), for $d/a = 0.3$ and 2.0, respectively. In addition to the $L_\pm$ dispersion curves, figure 6(*a*) also shows the dispersion curves of the $T_\pm$ modes. At the low value of d/a the frequencies of both the L_- and T_- out-of-phase modes exhibit a weak dependence on wave number k over the whole domain as shown in figure 6(*a*). This behaviour is in agreement with the predictions of the QLCA theory. On the other hand, the present simulations yield a $\approx$30% higher frequency of the out-of-phase modes at $k \to 0$ compared to the QLCA.

For the in-phase longitudinal mode L_+ the RPA theory predicts that for $k \to 0$ the dispersion is 2D-like $\omega \sim \sqrt{k}(1 - kd/2 + 3ka/4\Gamma)$, while the QLCA predicts a further $O(k)$ correction due to particle correlations [24, 26, 35]. Our simulation results reproduce this latter behaviour; the RPA results increasingly deviate from the present data as ka increases. The in-phase transverse T_+ mode is quite weak for $\Gamma = 40$, similar to the behaviour of the corresponding mode in the isolated 2D system where, however, the mode becomes stronger at higher values of Γ [36]. Here the T_+ mode is observable only at wave numbers $ka \geqslant 1$; for $ka \leqslant 1$, $\omega = 0$. The disappearance of the shear modes for $k \to 0$ is a well-known feature of the liquid state [36–38]; the sharp cut-off, $\omega \to 0$ for a finite k, has also been observed in simulations of Yukawa systems [39, 40]. Comparison with the QLC theory shows an agreement as far as the linear acoustic dispersion is concerned, but the QLCA fails to predict the finite k, $\omega = 0$ cut-off.

At high layer separations, as shown in figure 6(*b*) for $d/a = 2.0$, the major portion of the out-of-phase longitudinal (L_-) mode at low wave numbers exhibits the linear acoustic behaviour predicted by the RPA. Figure 6(*b*) also shows the result of the QLC theory calculation at $d/a = 2.0$ [26], which is in good agreement with the present MD results.

The widths of the peaks in the fluctuation spectra are related to the lifetimes of the corresponding modes. $L_+(\omega)$, which is maintained primarily by the mean field, is characterized by an extremely narrow peak and a long lifetime. In contrast, $T_+(\omega)$ and $T_-(\omega)$, which are supported by particle correlations, have broader peaks and shorter lifetimes. The peak for $L_-(\omega)$ is broad in the domain dominated by correlations (low d/a), in particular in the gap region; it narrows dramatically, however, as it travels into the quasi-linear region (high d/a) which again is maintained primarily by the mean field.

5. Summary

In this paper, we have reviewed the results of MD simulations of strongly coupled, classical charged particle bilayer liquids. The simulations confirm a sequence of structural changes in the liquid phase, induced by the changing separation of the two layers. The intralayer and interlayer pair correlation functions have made it possible to calculate the energy of the system, as well as the static structure functions. The structure functions have been found to satisfy the perfect screening sum rule $S_{11}(k = 0) = -S_{12}(k = 0) = S_0$.

The dynamical simulations have generated current fluctuation spectra. From the analysis of these spectra we have identified the four collective modes of the system and have determined their dispersion characteristics. The existence of a frequency (energy) gap in the out-of-phase modes has been unambiguously established. The qualitative conclusions of the QLCA for all four modes, in particular those concerning the emergence of the energy gap for the out-of-phase modes, are verified. Quantitatively, the agreement between the MD and the QLCA results is excellent for the in-phase longitudinal mode; for the out-of-phase modes the value of the energy gap obtained in the present work is about 30% higher than that predicted by the QLCA. The reason for this discrepancy is not understood at the present time. The MD results well complement the existing experimental findings [41] in laboratory experiments that have been carried out for $r_s \approx 1.0$–1.5, a much weaker coupling range than that investigated in the present simulations.

Acknowledgments

ZD thanks Satoshi Hamaguchi (University of Kyoto) and GJK thanks Harvey Gould, Krastan Blagoev and Stamatios Kyrkos for useful discussions. This work has been partially supported by grants MTA-OTKA-NSF-28, OTKA-T-34156, NSFINT-0002200, DE-FG02-98ER54501, DE-FG02-98ER54491, NSF PHY-0206695 and NSF PHY-0206554.

References

[1] Mitchell T B, Bollinger J J, Dubin D H E, Huang X-P, Itano W M and Bundham R H 1998 *Science* **282** 1290
[2] Bollinger J J, Mitchell T B, Huang X-P, Itano W M, Tan J N, Jelenković B M and Wineland D J 2000 *Phys. Plasmas* **7** 7
[3] Shapira S, Sivan U, Solomon P M, Buchstab E, Tischler M and Ben Yosef G 1996 *Phys. Rev. Lett.* **77** 3181
Kainth D S, Richards D, Bhatti A S, Hughes H P, Simmons M Y, Linfield E H and Ritchie D A 1999 *Phys. Rev.* B **59** 2095
[4] Rapisada F and Senatore G 1998 *Strongly Coupled Coulomb Systems* ed G J Kalman, K Blagoev and M Rommel (New York: Plenum)
[5] Millard I S, Patel N K, Simmons M Y, Linfield E H, Ritchie D A, Jones G A C and Pepper M 1996 *Appl. Phys. Lett.* **68** 3323
[6] Melzer A, Schweigert V A, Schweigert I V, Homann A, Peters S and Piel A 1996 *Phys. Rev.* E **54** R46
[7] Pieper J B, Goree J and Quinn R A 1996 *J. Vac. Sci. Technol.* **14** 519
[8] Nunomura S, Samsonov D and Goree J 2000 *Phys. Rev. Lett.* **84** 5141
[9] Rosenberg M 2000 *J. Phys. IV France* **10** Pr5-73
[10] Valtchinov V I, Kalman G J and Blagoev K B 1997 *Phys. Rev.* E **56** 4351
[11] Valtchinov V I, Kalman G J and Golden K I 1998 *Strongly Coupled Coulomb Systems* ed G J Kalman, K B Blagoev and M Rommel (New York: Plenum) p 533
[12] Kalman G J, Valtchinov V I and Golden K I 1998 *Condensed Matter Theories* vol 13 ed J Providencia and F B Malik (New York: Nova) p 209
[13] Kalman G J, Blagoev K B, Donkó Z, Golden K I, McMullan G, Valtchinov V and Zhao H 2000 *J. Phys. IV France* **10** Pr5-85

[14] Kalman G J, Donkó Z, Golden K I and McMullan G 2001 *Condensed Matter Theories* vol 16 ed S Hernandez, J Clark and B Malik (New York: Nova) p 51
[15] Baus M and Hansen J-P 1980 *Phys. Rep.* **59** 1
[16] Ichimaru S 1982 *Rev. Mod. Phys.* **54** 1017
[17] Goldoni G and Peeters F M 1996 *Phys. Rev.* B **53** 4591
[18] Weis J-J, Levesque D and Jorge S 2001 *Phys. Rev.* B **63** 045308
[19] Lado F 1978 *Phys. Rev.* B **17** 2827
[20] Schweigert I V, Schweigert V A and Peeters F M 1999 *Phys. Rev. Lett.* **82** 5293
[21] Schweigert I V, Schweigert V A and Peeters F M 2000 *J. Phys. IV France* **10** Pr5-117
[22] Donkó Z and Kalman G J 2001 *Phys. Rev.* E **63** 061504
[23] Ranganathan S, Johnson R E and Pathak K N 2002 *Phys. Rev.* E **65** 051203
[24] Das Sarma S and Madhukar A 1981 *Phys. Rev.* B **23** 805
[25] Kalman G J and Golden K I 1990 *Phys. Rev.* A **41** 5516
Golden K I and Kalman G J 2000 *Phys. Plasmas* **7** 14
[26] Kalman G J, Valtchinov V and Golden K I 1999 *Phys. Rev. Lett.* **82** 3124
[27] Ortner J 1999 *Phys. Rev.* B **59** 9870
[28] Golden K I and Kalman G J 2003 *J. Phys. A: Math. Gen.* **36** 5865–75
[29] Tkachenko I and Kalman G J 2000 *Proc. 10th Int. Conf. on the Physics of Nonideal Plasmas (Greifswald, Germany)*
[30] Ballester D, Kalman G J, Tkachenko I M and Zhang H 2003 *J. Phys. A: Math. Gen.* **36** 5887–92
[31] Donkó Z, Kalman G J, Hartmann P, Golden K I and Kutasi K Structure functions, collective mode dispersion, and energy gap in charged-particle bilayers (to be submitted)
[32] Hockney R W and Eastwood J W 1981 *Computer Simulation using Particles* (New York: McGraw-Hill)
[33] Hamaguchi S 1999 *Plasmas Ions* **2** 57
[34] Gann R C, Chakravarty S and Chester G V 1979 *Phys. Rev.* B **20** 326
[35] Vitlina R Z and Chaplik A V 1981 *Zh. Eksp. Teor. Fiz.* **81** 1011 (Engl. transl. *Sov. Phys.–JETP* **54** 536)
[36] Totsuji H and Kakeya N 1980 *Phys. Rev.* A **22** 1220
[37] Hansen J-P, McDonald I R and Pollock E L 1975 *Phys. Rev.* A **11** 1025
[38] Schmidt P, Zwicknagel G, Reinhard P-G and Toepffer C 1997 *Phys. Rev.* E **56** 7310
[39] Ohta H and Hamaguchi S 2000 *Phys. Rev. Lett.* **84** 6026
[40] Murillo M S 2000 *Phys. Rev. Lett.* **85** 2514
[41] Bolcatto P G and Proetto C R 2000 *Phys. Rev. Lett.* **85** 1734
Millard I S *et al* 1996 *Appl. Phys. Lett.* **68** 3323
Kainth D S, Richards D, Bhatti A S, Hughes H P, Simmons M Y and Ritchie D A 1999 *Phys. Rev.* B **59** 2095